JOC Article
pubs.acs.org/joc

Functionalized Thiophene-Based [7]Helicene: Chirooptical Properties versus Electron Delocalization

Andrzej Rajca,*,† Maren Pink,‡ Shuzhang Xiao,† Makoto Miyasaka,† Suchada Rajca,† Kausik Das,† and Kristin Plessel†

†Department of Chemistry, University of Nebraska, Lincoln, Nebraska 68588-0304, and ‡IUMSC, Department of Chemistry, Indiana University, Bloomington, Indiana 47405-7102

arajca1@unl.edu

Received August 16, 2009

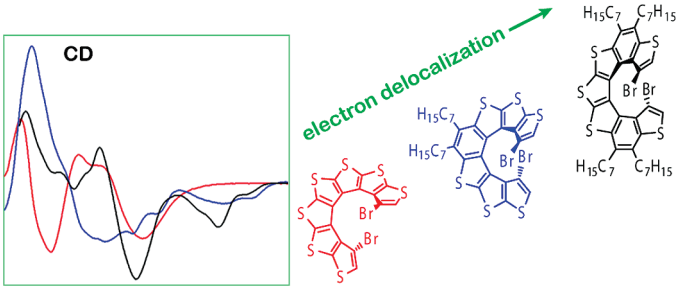

The functionalized, enantiomerically pure [7]helicene **1** derived from bis(benzodithiophene) functionalized with four heptyl groups is prepared from 1,8-dibromo-4,5-diheptylbenzo[1,2-*b*:4,3-*b*′]dithiophene building block **2**. Such [7]helicene structure, functionalized with bromines at the terminal positions of the helicene inner rim and multiple solubilizing alkyl groups, is an attractive building block for long [*n*]helicenes and oligo[7]helicenes. Chirooptical properties and the degree of electron delocalization are determined and compared to those of analogous carbon−sulfur [7]helicene and [7]helicenes derived from benzodithiophene to provide a correlation between chirooptical properties and the degree of electron delocalization. [7]Helicene **1** possesses a moderately increased electron delocalization, but its chirooptical properties are similar to those for analogous [7]helicenes with relatively lower electron delocalization, indicating that chirooptical properties are not significantly affected by electron delocalization for this series of [7]helicenes. Molecular structures of racemic [7]helicene **1** and its benzodithiophene building block **2** are confirmed by single-crystal X-ray analysis. Crystals of **2** are chiral and adopt the shape of long, flexible, flat needles that can be readily bent.

Introduction

Helical molecules and supramolecular assemblies are attractive building blocks for the development of materials with novel optical, electronic, and medicinal properties.[1−11] [*n*]Helicenes, the structures with *n ortho*-fused aromatic rings, are among the molecules with inherently strongest chiral properties, due to helical shape of their π-conjugated systems.[12−15] In recent years, there has been a surge of

(1) *Topics in Current Chemistry*; Crego-Calama, M., Reinhoudt, D. N., Eds.; Springer: Berlin, 2006; Vol. 265, pp 1−312.
(2) Hecht, S. *Mater. Today* **2005**, *8*, 48–55.
(3) Mishra, A.; Ma, C.-Q.; Bäuerle, P. *Chem. Rev.* **2009**, *109*, 1141–1276.
(4) Rajca, A.; Miyasaka, M. Synthesis and Characterization of Novel Chiral Conjugated Materials. In *Functional Organic Materials−Syntheses and Strategies*; Mueller, T. J. J., Bunz, U. H. F., Eds.; Wiley-VCH: New York, 2007; Chapter 15, pp 543−577.
(5) Katz, T. J. *Angew. Chem., Int. Ed.* **2000**, *39*, 1921–1923.
(6) (a) Verbiest, T.; Van Elshocht, S.; Kauranen, M.; Hellemans, L.; Snauwaert, J.; Nuckolls, C.; Katz, T. J.; Persoons, A. *Science* **1998**, *282*, 913–915. (b) Nuckolls, C.; Katz, T. J.; Katz, G.; Collings, P. J.; Castellanos, L. *J. Am. Chem. Soc.* **1999**, *121*, 79–88. (c) Phillips, K. E. S.; Katz, T. J.; Jockusch, S.; Lovinger, A. J.; Turro, N. J. *J. Am. Chem. Soc.* **2001**, *123*, 11899–11907. (d) Vyklický, L.; Eichhorn, S. H.; Katz, T. J. *Chem. Mater.* **2003**, *15*, 3594–3601.
(7) (a) Field, J. E.; Muller, G.; Riehl, J. P.; Venkataraman, D. *J. Am. Chem. Soc.* **2003**, *125*, 11808–11809. (b) Hassey, R.; Swain, E. J.; Hammer, N. I.; Venkataraman, D.; Barnes, M. D. *Science* **2006**, *314*, 1437–1439. (c) Cohen, A.; Tang, Y. *J. Phys. Chem. A* **2009**, *113*, 9759.
(8) Bossi, A.; Licandro, E.; Maiorana, S.; Rigamonti, C.; Righetto, S.; Stephenson, G. R.; Spassova, M.; Botek, E.; Champagne, B. *J. Phys. Chem. C* **2008**, *112*, 7900–7907.

Published on Web 09/09/2009 DOI: 10.1021/jo901769c

reports on the new synthesis of highly annelated helical structures, including new heterohelicenes.[15−24] The focus has been mainly on the challenge associated with developing new methods for the preparation of helicenes and their asymmetric syntheses.[16,17,20−23] However, poor solubility and scarcity of adequately functionalized building blocks become a formidable problem in the syntheses of long helicenes, as highly rigid, annelated structures offer rather limited options for adequate functionalization with solubilizing groups.[25−27]

Chiral properties of [*n*]helicenes tend to increase significantly with the number of *ortho*-fused rings (*n*).[28] An analogous correlation is well established for achiral π-systems for which optical properties are significantly enhanced with increased electron delocalization.[29−32] Therefore, long [*n*]helicenes are promising targets in our quest for materials with the strongest molecular chiral properties.[4,15b] Because of the difficult synthesis of long [*n*]helicenes, we explore the optimization of chirooptical properties for [*n*]helicenes with moderate value of *n*. In the series of [7]helicenes, we discern an important question whether there is a correlation between chirooptical properties and electron delocalization in the helical π-systems.

The cross-conjugated carbon−sulfur [*n*]helicenes possess the highest optical band gap, $E_g \approx 3.5$ eV, while the conjugated thia[*n*]helicenes with alternating thiophene and benzene rings possess the lowest, $E_g \approx 2.4$ eV, among the oligomers with configurationally stable helical π-systems (Figure 1).[3,15b,33,34]

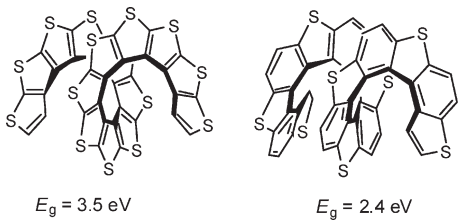

FIGURE 1. Optical band gaps (E_g) in cross-conjugated carbon−sulfur [*n*]helicenes and conjugated thia[*n*]helicenes with alternating thiophene and benzene rings.

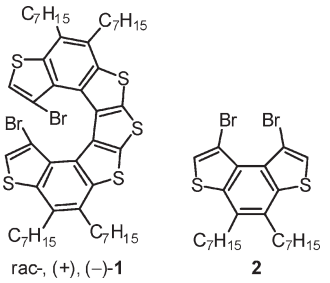

FIGURE 2. [7]Helicene **1** and 1,8-dibromo-4,5-diheptylbenzo[1,2-*b*:4,3-*b*′]dithiophene **2**.

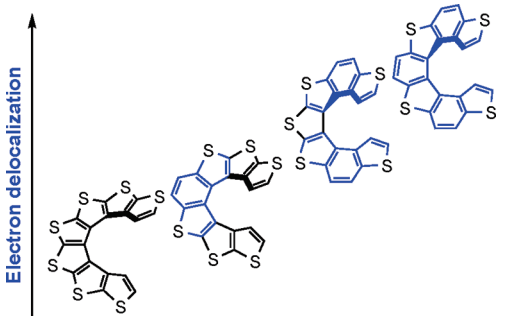

FIGURE 3. Generic [7]helicenes with increasing electron delocalization.

A systematic comparison of chirooptical properties of these helical π-systems with various degrees of electron delocalization would be highly valuable and of great interest in the design of materials with the strongest possible chiral properties.

Herein, we report the synthesis and study of a new functionalized, enantiomerically pure [7]helicene **1** derived from benzodithiophene building block **2** (Figure 2). [7]Helicene **1**, functionalized with bromines at the terminal positions of the helicene inner rim and multiple solubilizing alkyl groups, is an attractive building block for long, thiophene-based [*n*]helicenes and oligo[7]helicenes.[3,4,35] We implement a modified synthetic route to the 1,8-dibromo-4,5-diheptylbenzo-[1,2-*b*:4,3-*b*′]dithiophene **2**, which could serve as a versatile building block for organic-based electronic materials.[3,36] In the chiral crystals of **2** all molecules possess the same handedness; remarkably the needles are very flexible and can readily be bent perpendicular to (0 0 1).

The enantiomerically pure [7]helicene **1** presents us with an avenue for investigating the effect of electron delocalization on chirooptical properties and thus establishing a correlation between electron delocalization and chirooptical properties in a series of [7]helicene structures with various degree electron delocalization (Figure 3).

(9) (a) Stone, M. T.; Fox, J. M.; Moore, J. S. *Org. Lett.* **2004**, *6*, 3317−3320. (b) Amemiya, R.; Yamaguchi, M. *Org. Biomol. Chem.* **2008**, *6*, 26–35.

(10) Wilson, J. N.; Steffen, W.; McKenzie, T. G.; Lieser, G.; Oda, M.; Neher, D.; Bunz, U. H. F. *J. Am. Chem. Soc.* **2002**, *124*, 6830–6831.

(11) (a) Zahn, S.; Swager, T. M. *Angew. Chem., Int. Ed.* **2002**, *41*, 4225–4230. (b) Satrijo, A.; Swager, T. M. *Macromolecules* **2005**, *38*, 4054–4057.

(12) Newman, M. S.; Lutz, W. B.; Lednicer, D. *J. Am. Chem. Soc.* **1955**, *77*, 3420–3421.

(13) Newman, M. S.; Lednicer, D. *J. Am. Chem. Soc.* **1956**, *78*, 4765–4770.

(14) Newman, M. S.; Darlak, R. S.; Tsai, L. *J. Am. Chem. Soc.* **1967**, *89*, 6191–6193.

(15) For recent reviews on synthesis of helicenes, see: (a) Reference 4. (b) Rajca, A.; Rajca, S.; Pink, M.; Miyasaka, M. *Synlett* **2007**, 1799–1822. (c) Collins, S. K.; Vachon, M. P. *Org. Biomol. Chem.* **2006**, *4*, 2518–2524. (d) Torroba, T.; García-Valverde, M. *Angew. Chem., Int. Ed.* **2006**, *45*, 8092–8096. (e) Urbano, A. *Angew. Chem., Int. Ed.* **2003**, *42*, 3986–3989.

(16) (a) Collins, S. K.; Grandbois, A.; Vachon, M. P.; Côté, J. *Angew. Chem., Int. Ed.* **2006**, *45*, 2923–2926. (b) Grandbois, A.; Collins, S. K. *Chem.—Eur. J.* **2008**, *14*, 9323–9329.

(17) (a) Míšek, J.; Teplý, F.; Stará, I. G.; Tichý, M.; Šaman, D.; Císarová, I.; Vojtíšek, P.; Starý, I. *Angew. Chem., Int. Ed.* **2008**, *47*, 3188–3191. (b) Sehnal, P.; Krausova, Z.; Teply, F.; Stará, I. G.; Starý, I.; Rulisek, L.; Saman, D.; Cisarova, I. *J. Org. Chem.* **2008**, *73*, 2074–2082. (b) Helicene dications: Adriaenssens, L.; Severa, L.; Scaronálová, T.; Císarcaronová, I.; Pohl, R.; Scaronaman, D.; Rocha, S. V.; Finney, N. S.; Pospíscaronil, L.; Slavíccaronek, P.; Teplý, F. *Chem.—Eur. J.* **2009**, *15*, 1072–1076.

(18) Racemic oligophenylenes with helical connectivity and low barriers for racemization: (a) Han, S.; Bond, A. D.; Disch, R. L.; Holmes, D.; Schulman, J. M.; Teat, S. J.; Vollhardt, K. P. C.; Whitener, G. D. *Angew. Chem., Int. Ed.* **2002**, *41*, 3223–3227. (b) Han, S.; Anderson, D. R.; Bond, A. D.; Chu, H. V.; Disch, R. L.; Holmes, D.; Schulman, J. M.; Teat, S. J.; Vollhardt, K. P. C.; Whitener, G. D. *Angew. Chem., Int. Ed.* **2002**, *41*, 3227–3230.

(19) Conjoined helicenes: Shiraishi, K.; Rajca, A.; Pink, M.; Rajca, S. *J. Am. Chem. Soc.* **2005**, *127*, 9312–9313.

(20) Carreño, M. C.; González-López, M.; Urbano, A. *Chem. Commun.* **2005**, 611–613.

(21) Rajca, A.; Wang, H.; Pink, M.; Rajca, S. *Angew. Chem., Int. Ed.* **2000**, *39*, 4481–4483.

(22) Rajca, A.; Miyasaka, M.; Pink, M.; Wang, H.; Rajca, S. *J. Am. Chem. Soc.* **2004**, *126*, 15211–15222.

SCHEME 1. Synthesis of [7]Helicene *rac*-1

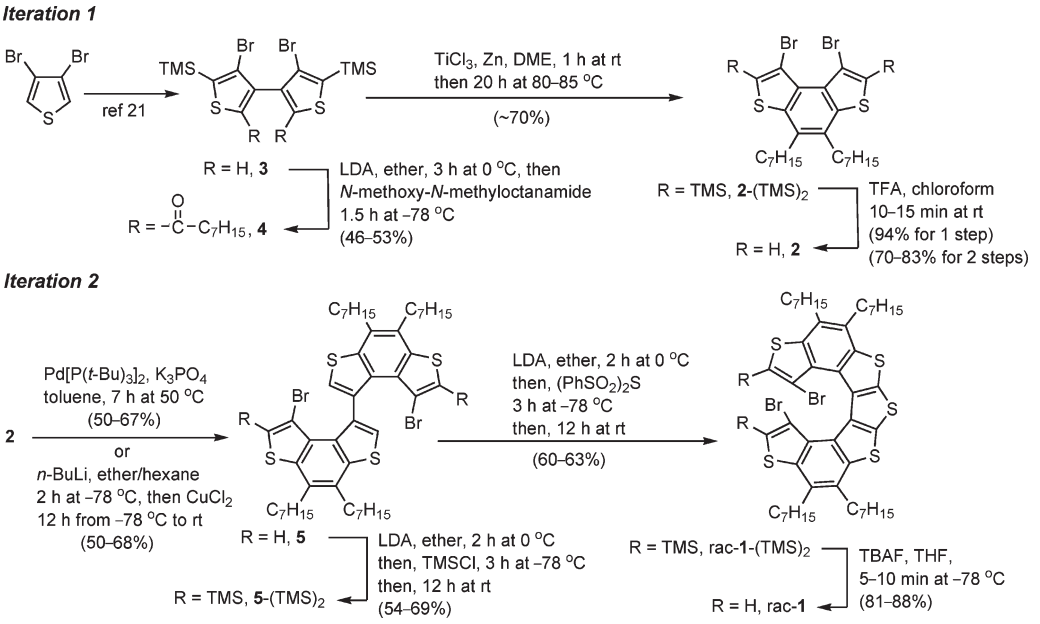

Results and Discussion

Racemic Synthesis of [7]Helicene 1. The synthesis of [7]helicene *rac*-**1** relies on two iterations of a sequence of connections of thiophene derivatives at their β-positions and annelation to form a thiophene or a benzene ring (Scheme 1).

In the first iteration, homocoupling of 3,4-dibromothiophene gives **3** as reported previously.[21,22] Dilithiation of **3** at the unprotected α-positions using lithium diisopropylamide (LDA) provides the resultant dilithiated derivative that subsequently reacts with *N*-methoxy-*N*-methyloctanamide to provide diketone **4**. The annelation step relies on the intramolecular McMurry reaction of diketone **4** using $TiCl_3-Zn$,[37,38] followed by removal of the TMS groups, to give benzodithiophene **2**.

In the second iteration, the connection step relies on a Pd-mediated reductive homocoupling reaction[23] or, alternatively, on a mono Li/Br exchange reaction of **2**, followed by oxidation of the resultant β-thienyllithium derivative with $CuCl_2$. Both methods give bis(benzodithiophene) **5** in similar yields. The excellent selectivity in the monohomocoupling reactions of dibromo-benzodithiophene **2** presumably originates from the close proximity in space of the two bromine atoms as observed in the X-ray structure of **2** (Figure 4). For comparison, the intramolecular Br···Br distance in the analogous 4,4′-dibromo-dithieno[2,3-*b*:3′,2′-*d*]thiophene is significantly longer, and thus its monohomocoupling reaction, based upon the Li/Br exchange, requires one of the bromine atoms to be sterically shielded with a TMS group at the α-position to attain good selectivity.[21,22] For the annelation step, the two most acidic α-positions in bis(benzodithiophene) **5** are protected with TMS to provide **5**-$(TMS)_2$, which is then annelated to [7]helicene *rac*-**1**-$(TMS)_2$. Deprotection of the TMS groups using tetrabutylammonium fluoride (TBAF) at low temperature gives the target [7]helicene *rac*-**1**.

(23) Miyasaka, M.; Rajca, A.; Pink, M.; Rajca, S. *J. Am. Chem. Soc.* **2005**, *127*, 13806–13807.
(24) Miyasaka, M.; Rajca, A.; Pink, M.; Rajca, S. *Chem.—Eur. J.* **2004**, *10*, 6531–6539.
(25) (a) Martin, R. H. *Angew. Chem., Int. Ed. Engl.* **1974**, *13*, 649–660. (b) [11], [12], and [14]helicenes: Martin, R. H.; Bayes, M. *Tetrahedron* **1975**, *31*, 2135–2137. (c) Martin, R. H.; Libert, V. *J. Chem. Res., Synop.* **1980**, 130–131.
(26) [7], [9], [11], [13], [15]Helicenes with alternate thiophene and benzene rings: Yamada, K.; Ogashiwa, S.; Tanaka, H.; Nakagawa, H.; Kawazura, H. *Chem. Lett.* **1981**, 343–346.
(27) Racemic [5], [7], [9], [11], [13]helicenes with alternate thiophene and benzene rings: (a) Larsen, J.; Bechgaard, K. *Acta Chem. Scand.* **1996**, *50*, 71–76. (b) Larsen, J.; Bechgaard, K. *J. Org. Chem.* **1996**, *61*, 1151–1152. (c) Caronna, T.; Catellani, M.; Luzatti; Malpezzi, L.; Meille, S. V.; Mele, A.; Richter, C.; Sinisi, R. *Chem. Mater.* **2001**, *13*, 3906–3914.
(28) Meurer, K. P.; Vögtle, F. *Top. Curr. Chem.* **1985**, *127*, 1–76.
(29) For naphthalene, anthracene, and tetracene, $\log(\varepsilon)$ for the longest wavelength bands (^1L_a) and second longest wavelength (^1B_b) increases with *n*, the number of annelated benzene rings: Klessinger, M.; Michl, J. *Excited States and Photochemistry of Organic Molecules*; VCH: New York, 1995; Chapter 2, pp 63–137.
(30) Oscillator strengths *f* of the longest wavelength absorption increases with the number *n* of double bonds and triple bonds in linear polyenes, cyanines, and related π-systems: Nayler, P.; Whiting, M. C. *J. Chem. Soc.* **1955**, 3037–3047. (b) Kuhn, H. *J. Chem. Phys.* **1958**, *29*, 958–959. (c) Mason, S. F. *Q. Rev. Chem. Soc.* **1961**, *15*, 287–371.
(31) Roncali, J. *Macromol. Rapid Commun.* **2007**, *28*, 1761–1775.
(32) (a) Moonen, N. N. P.; Pomerantz, W. C.; Gist, R.; Boudon, C.; Gisselbrecht, J.-P.; Kawai, T.; Kishioka, A.; Gross, M.; Irie, M.; Diederich, F. *Chem.—Eur. J.* **2005**, *11*, 3325–3341. (b) Pilzak, G. S.; Baggerman, J.; Lagen, B.; Posthumus, M. A.; Sudhölter, E. J. R.; Zuilhof, H. *Chem.—Eur. J.* **2009**, *15*, 2296–2304.
(33) The band gaps based upon extrapolation of the calculated B3LYP-6-31G(d) HOMO–LUMO gaps are 4.1, 2.5, and 2.9 eV for cross-conjugated carbon–sulfur [*n*]helicenes, conjugated [*n*]helicenes with alternating thiophene and benzene rings, and conjugated all-benzene [*n*]helicenes, respectively: Tian, Y.-H.; Park, G.; Kertesz, M. *Chem. Mater.* **2008**, *20*, 3266–3277.
(34) [*n*]Helicenes composed of benzene rings, possessing conjugated systems, have an estimated band gap of 2.5 eV, based upon extrapolation of experimental UV–vis absorption spectra (ref 15b).
(35) Miyasaka, M.; Pink, M.; Rajca, S.; Rajca, A. *Angew. Chem., Int. Ed.* **2009**, *48*, 5954–5957.
(36) (a) Tanaka, K.; Osuga, H.; Tsujiuchi, N.; Hisamoto, M.; Sasaki, Y. *Bull. Chem. Soc. Jpn.* **2002**, *75*, 551–557. (b) Nishide, Y.; Osuga, H.; Saito, M.; Aiba, T.; Inagaki, Y.; Doge, Y.; Tanaka, K. *J. Org. Chem.* **2007**, *72*, 9141–9151. (c) Xiao, S.; Zhou, H.; You, W. *Macromolecules* **2008**, *41*, 5688–5696.
(37) McMurry, J. E. *Chem. Rev.* **1989**, *89*, 1513–1524.
(38) Fürstner, A.; Hupperts, A.; Ptock, A.; Janssen, E. *J. Org. Chem.* **1994**, *59*, 5215–5229.

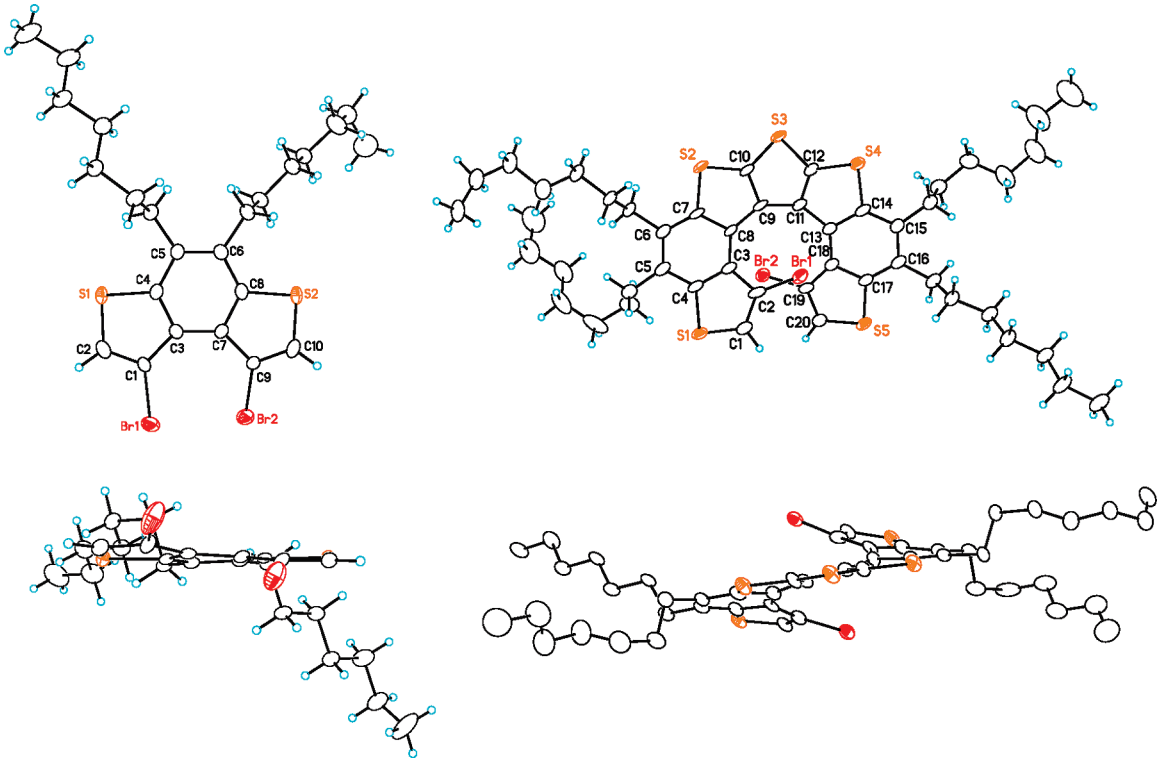

FIGURE 4. Molecular structures of **2** (left) and *rac*-**1** (right). The top and side views of the Ortep plots at 50% probability levels are shown for each molecule. Disorder of heptyl chains is omitted for clarity.

SCHEME 2

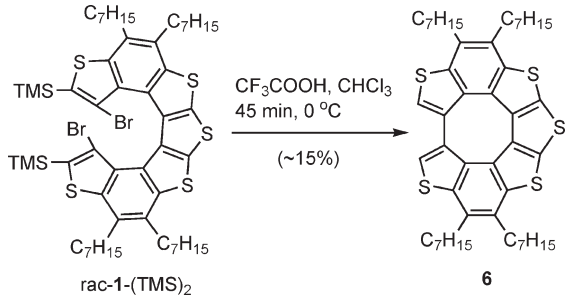

The deprotection method using trifluoroacetic acid is effective for the removal of TMS groups at α-positions in analogous [7]helicenes (and in **2**-$(TMS)_2$).[21−23,39] However, this method yields complex reaction mixtures when applied to *rac*-**1**-$(TMS)_2$.[40] Under anaerobic conditions, product **6** is isolated in low yield (Scheme 2).[40,41]

Resolution of [7]Helicene *rac*-1. The resolution method developed for carbon−sulfur [7]helicene is adapted to [7]helicene *rac*-**1**.[22] Treatment of *rac*-**1** with LDA is followed by treatment of the resultant α,α′-dilithiated derivative with chiral chlorosiloxane (−)-MenthSiCl. The mixture of diastereomeric disiloxanes was separated by column or preparative thin layer chromatography (silica gel, pentane/benzene, 15:1) to provide (−)-**7** (R_f = 0.40) and (+)-**7** (R_f = 0.30). The removal of the siloxanes using TBAF yields [7]helicenes (−)-**1** and (+)-**1** with good yield and good enantiomeric purity (Scheme 3).

Crystal Structures. Structures of *rac*-**1** and **2** were confirmed by single-crystal X-ray analysis (Figure 4 and Table S1 in Supporting Information). For *rac*-**1**, synchrotron radiation was required, because only relatively small, low-quality crystals of *rac*-**1** were available.[42]

In benzodithiophene **2**, the peripheral bromine atoms may not be accommodated in a planar geometry. Consequently, the π-system of **2** adopts the shape of a helix, with a turn angle of 137° and inner (C1, C3, C7, C9) helix climb of 0.46 Å.[43,44] The C−Br bonds are twisted out-of-plane as indicated by the Br1−C1−C9−Br2 torsion angle of 32.20(14)°.[44] The Br1···Br2 distance of 3.3223(6) Å is less than the sum of the van der Waals radii of 3.7 Å.

The structure of [7]helicene *rac*-**1** has an approximate C_2 symmetry. The Br1···Br2 distance is 4.5262(11) Å, significantly longer than that in **2**. The Br1−C2−C19−Br2 torsion angle is −146.16(27)°. The helix of **1** is remarkably flattened, compared to those of analogous thiophene-based [7]helicenes; with the

(39) Miyasaka, M.; Rajca, A. *J. Org. Chem.* **2006**, *71*, 3264–3266.

(40) (a) Das, K. *Ph.D. Dissertation*, University of Nebraska, Lincoln, **2007**; http://digitalcommons.unl.edu/dissertations/AAI3271933. (b) Figure S46 and Table S8, Supporting Information.

(41) Rajca, A.; Miyasaka, M.; Xiao, S.; Boratyński, P.; Pink, M.; Rajca, S. Manuscript in preparation.

(42) In the X-ray structure of [7]helicene *rac*-**1**, relatively high residual electron densities near bromine and sulfur atoms remained unassigned. We postulate that these are artifacts from multiply twinned crystal, that is, in addition to the major domain that was used to integrate the data, multiple minor domains were indexed; however, they could not satisfactorily be included in the data reduction. Consequently, variations for chemically equivalent bond lengths and angles and higher than usual standard uncertainties are found. Nevertheless, the X-ray data provide unequivocal confirmation of the structure for *rac*-**1** and a reasonably accurate helix shape.

(43) For calculations of overall helix structure for helicenes, see: Navaza, I.; Tsoucaris, G.; Le Bas, G.; Navaza, A.; de Rango, C. *Bull. Soc. Chim. Belg.* **1979**, *88*, 863–870.

(44) For **2**, mean deviation from a calculated least-squares plane including two bromines, benzene ring, and two thiophene rings (Br1, Br2, S1, S2, C1−C10) is 0.0781 Å. The C1−C3−C7−C9 torsion angle (along the inner helix) is 12.8(7)°.

SCHEME 3. Resolution of [7]Helicene 1

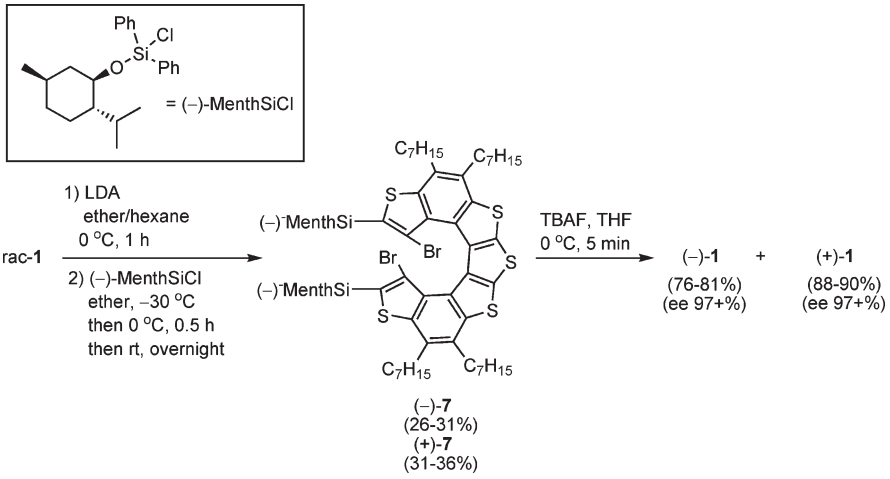

middle thiophene ring as a reference, the inner (C2, C3, C8, C9, C11, C13, C18, C19) helix climbs only 2.62 Å and turns in-plane by 287° (Table 2).

Crystal Packing. Benzodithiophene **2** crystallizes in the chiral space group $P2_1$. All molecules possess helically distorted π-system of identical handedness. The π-systems of **2** slip-stack, with plane-to-plane distance of 3.574 Å,[45] forming π-stacked columns along the crystallographic *b*-axis. The columns adopt herringbone-like orientation along the crystallographic *a*-axis, with two nonclassical hydrogen bonds, C2−H2···S1, for each pair of the nearest neighbor molecules in the adjacent columns. The heptyl chains are interdigitated along the crystallographic *a*- and *c*-axes (Figure 5).

The crystals of **2** grow as long, flat, flexible needles, which appear to consist of yet smaller needles, and can readily be bent (Figure 6 and Figure S11, Supporting Information).[46,47] The diffraction pattern showed peaks broadened in *b**, consistent with the morphology observed; the short crystallographic axis (*b*) corresponds to the long side of the needle. The propensity of the crystal for bending in the direction perpendicular to (0 0 1) may be explained by anisotropic crystal packing.[48] Specifically, bending is facile in the direction of weak van der Waals interactions between interdigitated heptyl chain, which is perpendicular to the direction of strong π-stacking interactions along the *b*-axis (Figure 5). Multiple bending attempts lead to disordered crystal packing as indicated by smeared diffraction patterns (Figure S12, Supporting Information). We postulate that in the process of flexing and bending the needle, the neighboring π-stacks become separated and eventually the 3-dimensional order of the packing is lost.

[7]Helicene *rac*-**1** crystallizes in the *P*-1 space group with 2 molecules of opposite configuration per unit cell. The crystal packing may be described in terms of tilted [7]helicenes with identical configurations forming columns along the *a*-axis; unlike for **2**, π-stacking is negligible. Approximately along the *c*-axis, the columns with [7]helicenes of opposite configurations form a one-dimensional network of short intermolecular S···S contacts: S1···S5 = 3.57 Å and S2···S3 = 3.58 Å, with four such contacts per molecule. The heptyl

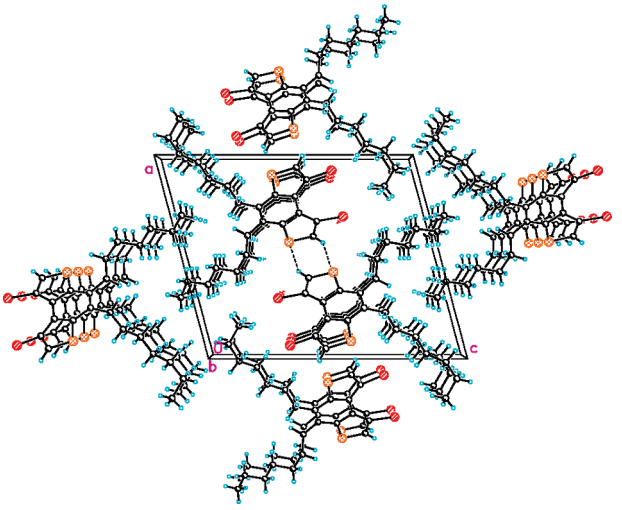

FIGURE 5. Crystal packing of **2**: view along crystallographic *b*-axis. Nonclassical hydrogen bonds are shown with dashed lines.

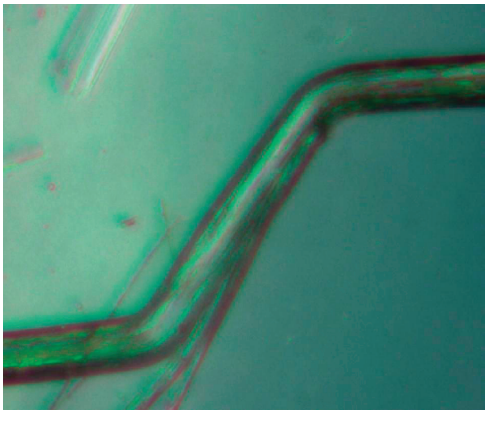

FIGURE 6. Crystal of **2** after bending.

(45) Distance between the least-squares planes, including benzene ring and two thiophene rings (S1, S2, C1−C10), for the adjacent molecules of **2** slip-stacked (π-stacked) along the *b*-axis.

(46) Propeller-shape molecule forming crystals with helical morphology: Ho, D. M.; Pascal, R. A., Jr. *Chem. Mater.* **1993**, *5*, 1358–1361.

(47) Bending of organic crystals upon irradiation: Koshima, H.; Naoko Ojima, N.; Uchimoto, H. *J. Am. Chem. Soc.* **2009**, *131*, 6890–6891.

(48) (a) Reddy, C. M.; Gundakaram, R. C.; Basavoju, S.; Kirchner, M. T.; Padmanabhan, K. A.; Desiraju, G. R. *Chem. Commun.* **2005**, 3945–3947. (b) Reddy, C. M.; Kirchner, M. T.; Gundakaram, R. C.; Padmanabhan, K. A.; Desiraju, G. R. *Chem.—Eur. J.* **2006**, *12*, 2222–2234.

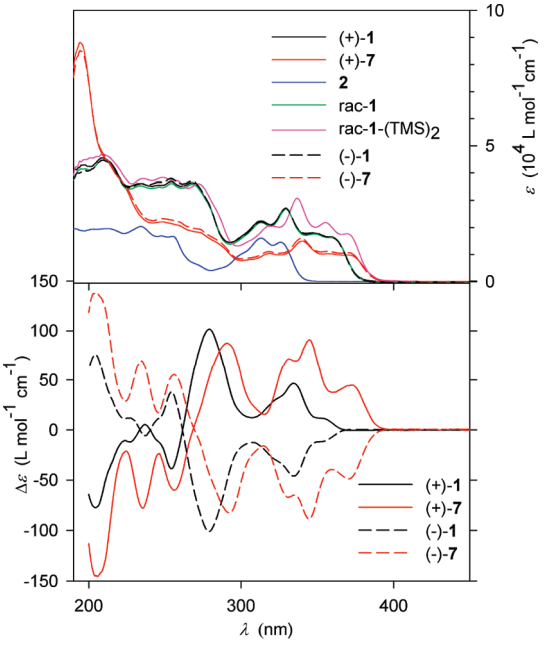

FIGURE 7. Electronic UV−vis spectra (top) and CD spectra (bottom) for [7]helicenes and benzodithiophene **2** in cyclohexane.

TABLE 1. Summary of Chirooptical Data for [7]Helicenes (−)-8, (+)-9, and (−)-1 in Cyclohexane

compound[a]	λ_{max}, nm (ε_{max}, L mol^{-1} cm^{-1})	λ_{max}, nm ($\Delta\varepsilon_{max}$, L mol^{-1} cm^{-1})	$[\alpha]^{rt}_D$	[Φ]
(−)-**1**	329 (2.7×10^4)	334 (−46)	−752	−7210
(−)-**7**	339 (1.6×10^4)	345 (−89)	−658	−10740
(−)-**8**[a]	246 (2.8×10^4)	283 (−61)	−1260	−7280
(+)-**9**[a]	353 (1.6×10^4)	337 (+22)	+1010	+7730

[a]Chirooptical data for (−)-**8** and (+)-**9** is from refs 22 and 24.

chains are interdigitated along the crystallographic *b*-axis (Figure S10, Supporting Information).

UV−vis and CD Spectroscopy. Electronic UV−vis and CD spectra for selected compounds in cyclohexane are shown in Figure 7.

The UV−vis spectra for [7]helicene (+)-, (−)-, and *rac*-**1** show bathochromic shifts throughout the recorded wavelength range, compared to that for benzodithiophene **2**. The silane and siloxane substitutents induce further bathochromic shifts in the long-wavelength bands for [7]helicenes *rac*-**1**-$(TMS)_2$ and (+)- and (−)-**7**. These bathochromic shifts are analogous to those in carbon−sulfur [7]helicenes.[22]

The CD spectra possess both spectral envelopes and absorbances analogous to typical conjugated helicenes.[4] Enantiomers (+)- and (−)-**1** give mirror image spectra, but also diastereomers (+)- and (−)-**7**, with (−)-menthol-based siloxane groups, have nearly mirror image spectra as well. These (+)-[7]helicenes with positive $[\alpha]_D$ possess positive sign of the longest wavelength CD band and vice versa, as found for previously reported helicenes. For the siloxane-substituted (+)- and (−)-**7**, the longest wavelength CD band shows a bathochromic shift of about 10 nm and possesses approximately double the intensity compared to that in (+)- and (−)-**1**. Consequently, the chirooptical properties for (−)-**7**, in particular molar rotation [Φ], are significantly enhanced (Table 1).

The correlation between chiroptical properties and the degree of electron delocalization is studied in the series of

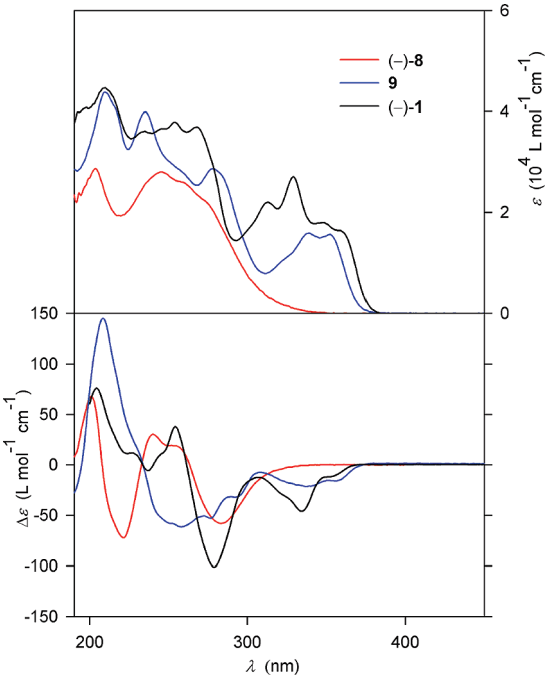

FIGURE 8. Electronic UV−vis spectra (top) and CD spectra (bottom) for [7]helicene (−)-**1**. The spectra for other [7]helicenes (−)-**8** and **9**, including the inverted CD spectrum for (*P*)-**9**, are shown for reference (structures in Chart 1).

CHART 1. Structures of Reference [7]Helicenes

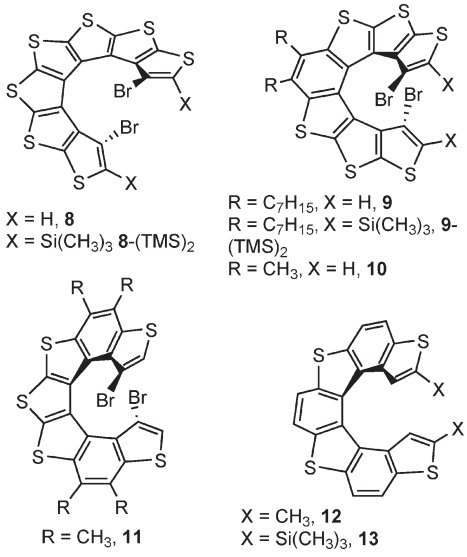

[7]helicenes **1**, **8**, and **9** (Chart 1, Table 1, Figure 8).[22,24] All-thiophene [7]helicene such as **8** possesses a cross-conjugated π-system, and therefore it serves as a reference with the least electron delocalization.[21−23,49−52] Compared to **8**, the UV−vis and CD spectra of [7]helicences with one and two benzene rings, **9** and **1**, show significantly different spectral

(49) Osuna, R. M.; Ortiz, R. P.; Hernández, V.; Navarrete, J. T.; Miyasaka, M.; Rajca, S.; Rajca, A.; Glaser, R. *J. Phys. Chem. C* **2007**, *111*, 4854–4860.
(50) Gholami, M.; Tykwinski, R. R. *Chem. Rev.* **2006**, *106*, 4997–5027.
(51) Nielsen, M. B.; Diederich, F. *Chem. Rev.* **2005**, *105*, 1837–1868.
(52) Absolute configuration for bis(trimethylsilyl)-substituted **8** has been reported: Friedman, T. B.; Cao, X.; Wang, H.; Rajca, A.; Nafie, L. A. *J. Phys. Chem. A* **2003**, *107*, 7692–7696.

TABLE 2. Summary of Overall Helix Structures

	X-ray structure				B3LYP/6-31G-(d,p) geometry		
	8-$(TMS_2)^a$	**9**-$(TMS)_2{}^a$	**9**^{a}	*rac*-**1**	**8**	**10**	**11**
climb (Å)	2.54	3.15	3.52	2.62	2.90	3.33	2.86
turn (deg)	262	311	305	287	271	310	288

[a]References 22 and 24.

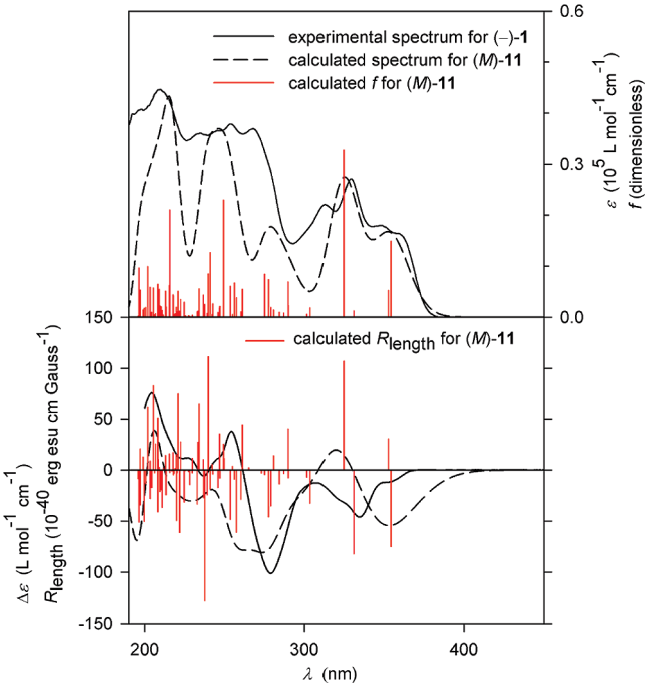

FIGURE 9. Electronic absorption UV−vis spectra (top) and CD spectra (bottom) for [7]helicene (−)-**1** in cyclohexane and calculated spectra for [7]helicene (*M*)-**11** at the TD-B3LYP/6-31G(d,p) level with the IEF-PCM-UAHF solvent model for cyclohexane. Calculated oscillator strengths, *f*, and rotary strengths, R_{length}, are shown as stick plots.

envelopes and bathochromic shifts. This suggests an increased degree of electron delocalization in **9** and **1**. However, the overall intensity of the long-wavelength CD bands does not significantly increase in **9** and **1**, compared to **8**, and consequently the chirooptical properties as measured by [Φ] are similar for all three [7]helicenes.

[7]Helicenes with alternating thiophene and benzene rings, such as **12** and **13** (Chart 1), should possess an even greater degree of electron delocalization, with their long-wavelength UV−vis and CD bands shifted to about 400 nm.[53,54] The molar rotation, [Φ] = 11700 (chloroform), for **12** is greater than that for **1**, **8**, and **9** but similar to that for siloxane-substituted [7]helicene **7** (Table 1). For another [7]helicene with alternating thiophene and benzene rings such as **13** (Chart 1), a rather low value of [Φ] = 4760 was reported.[54] Thus, increased electron delocalization in the helical π-system of [7]helicenes does not enhance chirooptical properties; however, substituent effects appear to be significant.[55]

Calculations of UV−vis and CD Spectra. The helical shape, absolute configuration, and electronic structure of [7]helicene (−)-**1** in solution is further characterized by computational modeling of experimental electronic CD and UV−vis absorption spectra.[56] To facilitate the computations, we calculated a simplified structure (*M*)-**11**, in which the heptyl chains are replaced with methyl groups (Chart 1). For comparison, simplified structures (*M*)-**10** (corresponding to [7]helicene (*M*)-**9**) and [7]helicene (*M*)-**8** were calculated as well (Chart 1).

Geometries for [7]helicenes (*M*)-**8**, (*M*)-**10**, and (*M*)-**11**, constrained to the C_2 point group, are optimized at the B3LYP/6-31G(d,p) level. Vibrational frequency calculations indicate that the resultant C_2-symmetric structures are minima on the potential energy surface. The overall helix structure at the optimized geometry for (*M*)-**11** is similar to that determined in [7]helicene *rac*-**1** by the X-ray analysis (Table 2); the BrCCBr torsion angles are 140.7° and 146.3°, and the Br···Br distances are 4.80 and 4.50 Å for (*M*)-**11** and *rac*-**1**, respectively.

Notably, both helical climb and helical turn angle first increases and then decreases in the series of [7]helicenes with the increasing number of benzene ring from 0 to 1 to 2. This trend is found both in the X-ray structures and in the calculated B3LYP/6-31G(d,p) geometries (Table 2), and therefore it is likely to be associated with the [7]helicene molecules and not crystal packing.

CD and UV−vis absorption spectra of [7]helicenes (*M*)-**8**, (*M*)-**10**, and (*M*)-**11** are calculated using the TD-B3LYP/6-31G(d,p) method and IEF-PCM-UAHF solvent model for cyclohexane.[56] The calculated spectra for (*M*)-**8**, (*M*)-**10**, and (*M*)-**11** are in qualitative agreement with the experimental spectra for (−)-**8**, (−)-**9**, and (−)-**1**, respectively (Figure 9 and Figure S7, Supporting Information). This result confirms the absolute configuration of (−)-**1** as *M*.

Conclusion

The syntheses of racemic and enantiopure, highly functionalized [7]helicene **1** provides a new building block for synthesis of long [*n*]helicenes and oligo[7]helicenes. Although [7]helicene **1** shows moderately increased electron delocalization as evidenced by significant bathochromic shift in the UV−vis absorption and CD spectra, its chirooptical properties are similar to those for analogous [7]helicenes with relatively lower electron delocalization, including carbon−sulfur [7]helicene with cross-conjugated π-system. Therefore, chirooptical properties are not significantly affected by electron delocalization for this series of [7]helicenes.

Experimental Section

Diketone 4. LDA solution in ether (0.48 M, 16.7 mL, 8.02 mmol, 2.4 equiv), which was prepared as described in Supporting Information, was added to a suspension of dithiophene **3**

(53) Tanaka, K.; Suzuki, H.; Osuga, H. *J. Org. Chem.* **1997**, *62*, 4465–4470.

(54) For TMS-substituted [7]helicene **13**, a rather low value of $[\alpha]_D$ = 870 (chloroform), corresponding to [Φ] = 4760, was reported, but the chirooptical data and determination of optical purity are deficient: Bossi, A.; Maiorana, S.; Graiff, C.; Tiripicchio, A.; Licandro, E. *Eur. J. Org. Chem.* **2007**, 4499–4509.

(55) For the most studied all-phenylene [6]helicenes, the relationship between the crystal structure (substituent-induced changes in helical shape) and optical rotation could not be established: Wachsmann, C.; Weber, E.; Czugler, M.; Seichter, W. *Eur. J. Org. Chem.* **2003**, 2863–2876.

(56) Frisch, M. J. et al. *Gaussian 03*, Revision E.01; Gaussian: Wallingford, CT, 2004.

(1.566 g, 3.34 mmol, 1.0 equiv) in ether (20 mL) at 0 °C. The nearly homogeneous, pale brown-orange reaction mixture was stirred for 3 h at 0 °C, and then *N*-methoxy-*N*-methyloctanamide (2.34 mL, 10.0 mmol, 3 equiv) was added dropwise (neat or as solution in ether) at −78 °C. After 1.5 h at −78 °C, the reaction mixture was poured into water. The usual aqueous workup with ether gave the crude product as an orange viscous liquid/oil. Column chromatography (silica, hexane/benzene, 1:1, v/v) of crude products from three reactions on 1.5, 1.5, and 3 g scales (total of 6.065 g of starting material **3**) gave 4.58 g (46−53%) of diketone **4**. R_f = 0.28 (hexane). Mp = 53−54 °C. ^{1}H NMR (400 MHz, chloroform-*d*): δ 2.43−2.24 (m, 4H), 1.63−1.44 (m, 4H, overlapped with H_2O peak), 1.32−1.05 (m, 16H), 0.851 (t, J = 7.2, 6H), 0.457 (s, 18H). ^{13}C{^{1}H} NMR (125 MHz, chloroform-*d*): δ 192.0 (C=O), aromatic region, expected 4 resonances; found 4 resonances at δ 144.7, 142.7, 140.3, 120.6; aliphatic region, expected 8 resonances; found 8 resonances at δ 40.0, 31.6, 29.1, 28.8, 23.9, 22.5, 14.0, −1.12 ($J(^{29}\mathrm{Si}-^{13}\mathrm{C})$ = 54 Hz). IR (ZnSe, cm^{-1}): 2955, 2925, 2855 (C−H), 1664 (C=O). HR FABMS (3-NBA matrix): m/z (ion type, % RA for m/z = 715−728, deviation for the formula): 721.1094 ([M + 2 + H]$^+$, 100%, −0.8 ppm for $^{12}C_{30}{}^1H_{49}O_2{}^{28}Si_2{}^{32}S_2{}^{79}Br^{81}Br$).

Benzodithiophene 2: Two-Step Procedure (Method C). Diketone **4** (0.577 g, 0.800 mmol, 1 equiv) in DME (55 mL) was added to a Schlenk vessel containing $TiCl_3$ (0.260 g, 1.69 mmol, 2.1 equiv) and Zn (0.274 g, 4.19 mmol, 5.2 equiv). The reaction mixture was stirred at ambient temperature for 1 h and then at 85−90 °C for 20 h. After cooling to ambient temperature, the reaction mixture (DME solution) was filtered through a silica plug, to provide **2**-(TMS)$_2$ as a pale yellow viscous oil (0.477 g, 87%, with 0.6% admixture of monodesilylated byproduct). Trifluoroacetic acid (1 mL) was added to a solution of this crude product (0.477 g) in chloroform (10 mL). After TLC analysis (hexane) indicated completion of the reaction, the usual aqueous workup with ether was carried out to provide the final crude product as a pale yellow solid. Filtration through a short silica plug using hexane gave **2** (0.337 g, 77% after 2 steps). R_f = 0.53 (hexane). Mp = 47−49 °C. ^{1}H NMR (500 MHz, chloroform-*d*): δ 7.564 (s, 2H), 2.99−2.92 (m, 4H), 1.73−1.64 (m, 4H), 1.52−1.43 (m, 4H), 1.42−1.26 (m, 12H), 0.901 (t, J = 7.2, 6H). ^{13}C{^{1}H} NMR (125 MHz, chloroform-*d*): aromatic region, expected 5 resonances; found 5 resonances at δ 142.3, 131.3, 129.6, 125.3, 105.3, aliphatic region, expected 7 resonances; found 7 resonances at δ 31.8, 31.4, 30.1, 29.6, 29.0, 22.7, 14.1. IR (ZnSe, cm^{-1}): 3095 (C−H of thiophene), 2955, 2923, 2855 (C−H). UV−vis (cyclohexane): λ_{max}/nm (ε/dm^3 mol^{-1} cm^{-1}) = 234 (2.03×10^4), 255 (1.67×10^4), 313 (1.59×10^4), 326 (1.44×10^4). HR FABMS (3-NBA matrix): m/z (ion type, % RA for m/z = 500−800, deviation for the formula): 544.0284 ([M + 2]$^+$, 100%, 1.4 ppm for $^{12}C_{24}{}^1H_{32}{}^{32}S_2{}^{79}Br^{81}Br$).

Bis(benzodithiophene) 5: Pd-Mediated Homocoupling Reaction. Benzodithiophene **2** (0.100 g, 0.18 mmol) and potassium phosphate (0.784 g, 0.37 mmol) were evacuated in high vacuum overnight in a Schlenk vessel. Subsequently, the Schlenk vessel was transferred to a glovebox, and then Pd[P(*t*-Bu)$_3$]$_2$ (0.94 g, 0.18 mmol) was added under argon atmosphere. Dry toluene (5 mL) was added under nitrogen atmosphere, and the resulting mixture was stirred at about 50 °C. After 7 h at about 50 °C, the reaction mixture was diluted with diethyl ether (20 mL) and washed with water (3 × 25 mL). The combined organic layers were dried over $MgSO_4$ and concentrated in vacuum to give a crude mixture as a yellow gel. Column chromatography (flash silica, hexanes) yielded the product as a yellow gel (0.052 g, 61%).

Bis(benzodithiophene) 5: $CuCl_2$-Mediated Homocoupling Reaction. *n*-BuLi (2.52 M in hexanes, 1.0 mL, 2.52 mmol, 1.05 equiv) was added to benzodithiophene **2** (1.331 g, 2.45 mmol, 1.0 equiv, evacuated overnight) in ether (100 mL) at −78 °C. After 2 h at −78 °C, $CuCl_2$ (0.986 g, 7.34 mmol, 3.0 equiv, dried in high vacuum at 80 °C overnight) was added to the solution of organolithium at −78 °C. Following the addition, the reaction mixure was allowed to attain room temperature overnight. After 20 h, the reaction mixture was washed with 6 M HCl (3 × 75 mL), saturated $NaHCO_3$ (2 × 75 mL), and water (75 mL). The combined organic layers were dried over $MgSO_4$ and concentrated in vacuo. Column chromatography provided homocoupling product **5** (0.741 g, 65%) as a yellow gel. R_f = 0.31 (hexane). ^{1}H NMR (500 MHz, chloroform-*d*): δ 7.349 (s, 2H), 7.189 (s, 2H), 3.08−2.94 (m, 8H), 1.81−1.72 (m, 8H), 1.56−1.50 (m, 8H, overlapped with the singlet peak of H_2O at δ 1.56 ppm), 1.43−1.37 (m, 8H), 1.35−1.32 (m, 16H), 0.916 (t, J = 7.5, 12H). ^{1}H NMR (400 MHz, chloroform-*d*): δ 7.348 (s, 2H), 7.190 (s, 2H), 3.09−2.93 (m, 8H), 1.83−1.69 (m, 8H), 1.61−1.49 (m, 2H, overlapped with H_2O at δ 1.56 ppm), 1.43−1.40 (m, 8H), 1.38−1.32 (m, 16H, overlapped with the peak of hexanes at δ 1.26 ppm), 0.914 (t, J = 6.8, 12H). ^{13}C{^{1}H} NMR (100 MHz, chloroform-*d*): aromatic region, expected 10 resonances; found 9 resonances at δ 141.5, 140.5, 137.2, 131.89, 131.45, 130.3, 124.9, 123.9, 106.5; aliphatic region, expected 14 resonances; found 12 resonances at δ 32.1 (br), 31.84, 31.82, 31.54 (br), 30.22, 30.19, 29.77, 29.72, 29.09, 29.08, 22.7, 14.1. IR (ZnSe, cm^{-1}): 3098 (α-C−H of thiophene), 2953, 2924, 2853 (C−H), 1466, 1251, 1160, 1102, 973, 748. HR FABMS (3-NBA matrix): m/z (ion type, % RA for m/z = 926−932, deviation for the formula): 928.2245 ([M + 2]$^+$, 100%, −0.9 ppm for $^{12}C_{48}{}^1H_{64}{}^{32}S_4{}^{79}Br_1{}^{81}Br_1$).

Bis(benzodithiophene) 5-(TMS)$_2$. The LDA solution in ether (0.31 M, 4.2 mL, 1.3 mmol) was added to **5** (0.562 g, 0.605 mmol) in ether (27 mL) at 0 °C. After 2 h at 0 °C, the reaction was placed in a −78 °C cooling bath, and then trimethylchlorosilane (0.23 mL, 1.8 mmol) was added. The resultant reaction mixture was allowed to warm to room temperature and was stirred for 20 h. The usual aqueous workup with ether provided crude product (0.622 g). The combined mixture of this crude product and another crude product (0.703 g), obtained from 0.634 g of **5**, was purified by column chromatography (TLC grade silica, hexane) to yield a total of 0.906 g (66%) of **5**-(TMS)$_2$ as a yellow gel. R_f = 0.46 (hexane). ^{1}H NMR (400 MHz, chloroform-*d*): δ 7.207 (s, 2H), 3.07−2.96 (m, 8H), 1.80−1.72 (m, 8H), 1.55−1.49 (m, 8H, overlapped with singlet at δ 1.516 from water), 1.44−1.38 (m, 8H), 1.36−1.32 (m, 16H, overlapped with multiplet of hexanes), 0.94−0.88 (m, 12H), 0.339 (s, 18H). ^{13}C{^{1}H} NMR (100 MHz, chloroform-*d*): aromatic region, expected 10 resonances; found 10 resonances at δ 143.2, 141.7, 137.9, 134.6, 133.0, 131.5, 131.2, 129.9, 124.2, 113.6, aliphatic region, expected 15 resonances; found 14 resonances at δ 31.95 (br), 31.90, 31.8, 31.3 (br), 30.21, 30.20, 29.78, 29.74, 29.13, 29.08, 22.73, 22.71, 14.2, −0.7. IR (ZnSe, cm^{-1}): 3095 (α-C−H of thiophene), 2954, 2925, 2854 (C−H), 1467, 1248, 841. HR FABMS (3-NBA matrix): m/z (ion type, % RA for m/z = 1070−1076, deviation for the formula): 1072.3052 ([M + 2]$^+$, 100%, −2.3 ppm for $^{12}C_{54}{}^1H_{80}{}^{28}Si_2{}^{32}S_4{}^{79}Br_1{}^{81}Br_1$).

[7]Helicene *rac*-1-(TMS)$_2$. A solution of LDA in ether (0.5 M, 0.24 mL, 0.12 mmol, 2.6 equiv) was added to **5**-(TMS)$_2$ (50.1 mg, 0.0467 mmol, 1.0 equiv) in ether (4.0 mL) at 0 °C. After 2 h at 0 °C, the reaction vessel was placed in a −78 °C bath, and then $(PhSO_2)_2S$ (25.0 mg, 0.079 mmol, 1.7 equiv) was added into the mixture. The resultant suspension was stirred at −78 °C for 3 h and then allowed to warm up to room temperature overnight. During the warm-up, the reaction mixture become clear (about 2 h at room temperature) and then turbid, with a large amount of yellow solid. Usual aqueous workup with hexane gave crude product (83.8 mg). A repeat reaction starting from 0.438 g of **5**-(TMS)$_2$ provided 0.841 g of crude product. Purification of the combined crude product by column chromatography (silica,

hexane) gave [7]helicene *rac*-**1**-$(TMS)_2$ as a yellow gel (0.294 g, 60%). R_f = 0.51 (hexane). ^{1}H NMR (400 MHz, chloroform-*d*): δ 3.13−2.89 (m, 8H), 1.80−1.69 (m, 8H), 1.55−1.48 (m, 8H, overlapped with the singlet peak of H_2O at δ 1.546 ppm), 1.46−1.37 (m, 8H), 1.34−1.26 (m, 16H), 0.95−0.88 (m, 12H), 0.228 (s, 18H). $^{13}C\{^1H\}$ NMR (100 MHz, chloroform-*d*): aromatic region, expected 10 resonances; found 10 resonances at δ 141.9, 141.4, 136.51, 136.35, 135.1, 133.4, 130.6, 130.1, 127.8, 114.9; aliphatic region, expected 15 resonances; found 14 resonances at δ 31.9, 31.84, 31.82, 30.9, 30.14, 30.07, 29.94, 29.7, 29.3, 29.1, 22.74, 22.68, 14.1, −0.8. IR (ZnSe, cm^{-1}): 2953, 2922, 2853 (C−H), 1467, 1450, 1247, 1016, 987, 841. UV−vis (cyclohexane): λ_{max}/nm (ε/dm^3 mol^{-1} cm^{-1}) = 272 (3.59 × 10^4), 319 (2.06 × 10^4), 337 (3.06 × 10^4), 355 (2.17 × 10^4), 369 (1.75 × 10^4). HR FABMS (3-NBA matrix, kd1360col3): *m*/*z* (ion type, % RA for *m*/*z* = 1099−1106, deviation for the formula): 1102.2614 ([M + 2]$^+$, 100%, −2.0 ppm for $^{12}C_{54}{}^1H_{78}{}^{28}Si_2{}^{32}S_5{}^{79}Br_1{}^{81}Br_1$).

Procedures for Deprotection of TMS and (−)-MenthSi Groups with TBAF: [7]Helicenes *rac*-1, (−)-1, and (+)-1. TBAF (1.0 M in THF, 0.68 mL, 0.68 mmol) was added under nitrogen atmosphere to [7]helicene *rac*-**1**-$(TMS)_2$ (0.288 g, 0.261 mmol) in THF (13 mL) at −78 °C. After 8 min at −78 °C, the reaction mixture was quenched with water 5 drops), and then usual aqueous workup with hexane was carried out. After removal of solvents in vacuo, crude product (0.491 g) was purified by column chromatography (deactivated silica, pentane) to provide [7]helicene *rac*-**1** as a pale yellow solid (0.212 g, 85%).

The deprotections of siloxane groups were carried out at 0 °C, using 20 equiv of TBAF in THF for 5 min. The usual workups with dichloromethane, followed by preparative TLC (deactivated silica, pentane), provided (−)-**1** (76−81%) and (+)-**1** (88−90%) as pale yellow or pale yellow-brown gels.

[7]Helicene *rac*-1. R_f = 0.35 (hexane). Mp = 99−101 °C. ^{1}H NMR (500 MHz, chloroform-*d*): δ 7.096 (s, 1H), 3.085−3.000 (m, 4H), 2.971−2.905 (m, 4H), 1.83−1.68 (m, 8H), 1.55−1.46 (m, 8H, overlapped with singlet at δ 1.548 from H_2O), 1.43−1.37 (m, 8H), 1.34−1.29 (m, 16H), 0.909 (LB = −1.87 Hz, GB = 0.53 Hz, t, *J* = 7, 6H), 0.907 (LB = −1.87 Hz, GB = 0.53 Hz, t, *J* = 7, 6H). $^{13}C\{^1H\}$ NMR (100 MHz, chloroform-*d*): aromatic region, expected 10 resonances; found 10 resonances at δ 141.6, 139.0, 136.9, 136.0, 132.7, 130.8, 130.3, 127.8, 122.3, 108.0; aliphatic region, expected 14 resonances; found 11 resonances at δ 31.95, 31.84, 31.81, 31.2, 30.12, 30.03, 29.94, 29.14, 29.10, 22.7, 14.3. IR (ZnSe, cm^{-1}): 3105 (α-C−H of thiophene), 2953, 2924, 2854 (C−H), 1466, 979, 739. UV−vis (cyclohexane): λ_{max}/nm (ε/dm^3 mol^{-1} cm^{-1}) = 210 (4.45 × 10^4), 268 (3.58 × 10^4), 313 (2.19 × 10^4), 329 (2.68 × 10^4), 348 (1.76 × 10^4). HR FABMS (3-NBA matrix): *m*/*z* (ion type, % RA for *m*/*z* = 954−963, deviation for the formula): 958.1825 ([M + 2]$^+$, 100%, −2.5 ppm for $^{12}C_{48}{}^1H_{62}{}^{32}S_5{}^{79}Br_1{}^{81}Br_1$).

[7]Helicene (−)-1. R_f = 0.35 (hexane). 98+ % ee (HPLC), $[\alpha]^{rt}_D$ = −750 (*c* 2.15 × 10^{-4} M, 0.21 mg/mL, cyclohexane). ^{1}H NMR (500 MHz, chloroform-*d*): δ 7.095 (s, 2H), 3.08−2.90 (m, 8H), 1.84−1.69 (m, 8H), 1.55−1.45 (m, 8H, overlapped with singlet peak of H_2O), 1.40−1.37 (m, 8H), 1.33−1.31 (m, 16H), 0.92−0.89 (t, *J* = 6.2, 12H). $^{13}C\{^1H\}$ NMR (125 MHz, chloroform-*d*): aromatic region, expected 10 resonances; found 10 resonances at δ 141.6, 139.0, 136.9, 136.0, 132.7, 130.8, 130.3, 127.8, 122.3, 107.9; aliphatic region, expected 14 resonances; found 11 resonances at δ 31.95, 31.84, 31.80, 31.2, 30.11, 30.03, 29.94, 29.14, 29.10, 22.7, 14.1. IR (ZnSe, cm^{-1}): 3107 (α-C−H of thiophene), 2954, 2923, 2853 (C−H), 1466. UV−vis (cyclohexane): λ_{max}/nm (ε/dm^3 mol^{-1} cm^{-1}) = 210 (4.44 × 10^4), 268 nm (3.71 × 10^4), 313 (2.20 × 10^4), 329 (2.71 × 10^4), 348 (1.79 × 10^4). CD (cyclohexane): λ_{max}/nm ($\Delta\varepsilon$/dm^3 mol^{-1} cm^{-1}): 334.2 (−46), 278.8 (−101), 254.2 (+38), 204.4 (+76). HR FABMS (3-NBA matrix): *m*/*z* (ion type, % RA for *m*/*z* = 955−963, deviation for the formula): 958.1763 ([M + 2]$^+$, 100%, 4.0 ppm for $^{12}C_{48}{}^1H_{62}{}^{32}S_5{}^{79}Br_1{}^{81}Br_1$).

[7]Helicene (+)-1. R_f = 0.35 (hexane). 99+ % ee (HPLC). $[\alpha]^{rt}_D$ = +790 (*c* 4.65 × 10^{-4} M, 0.45 mg/mL, cyclohexane). ^{1}H NMR (500 MHz, chloroform-*d*): δ 7.095 (s, 2H), 3.08−2.90 (m, 8H), 1.81−1.68 (m, 8H), 1.53−1.45 (m, 8H, overlapped with singlet peak of H_2O), 1.41−1.38 (m, 8H), 1.34−1.31 (m, 16 H), 0.92−0.89 (t, *J* = 6.5, 12H). $^{13}C\{^1H\}$ NMR (125 MHz, chloroform-*d*): aromatic region, expected 10 resonances; found 10 resonances at δ 141.6, 139.0, 136.9, 136.0, 132.7, 130.8, 130.3, 127.8, 122.3, 107.9; aliphatic region, expected 14 resonances; found 11 resonances at δ 31.95, 31.84, 31.80, 31.2, 30.11, 30.03, 29.94, 29.14, 29.10, 22.7, 14.1. IR (ZnSe, cm^{-1}): 3107 (α-C−H of thiophene), 2954, 2924, 2854 (C−H), 1466. UV−vis (cyclohexane): λ_{max}/nm (ε/dm^3 mol^{-1} cm^{-1}) = 210 (4.51 × 10^4), 268 (3.65 × 10^4), 313 (2.23 × 10^4), 329 (2.69 × 10^4), 348 (1.78 × 10^4). CD (cyclohexane): λ_{max}/nm ($\Delta\varepsilon$/dm^3 mol^{-1} cm^{-1}): 334.2 (+46), 279.2 (+102), 254.2 (−39), 204.4 (−77). HR FABMS (3-NBA matrix): *m*/*z* (ion type, %RA for *m*/*z* = 955−963, deviation for the formula): 958.1791 ([M + 2]$^+$, 100%, 1.0 ppm for $^{12}C_{48}{}^1H_{62}{}^{32}S_5{}^{79}Br_1{}^{81}Br_1$).

[7]Helicenes (−)-7 and (+)-7. A solution of LDA in ether (0.25 M, 0.12 mL, 0.0283 mmol, 2.3 equiv) was added dropwise to [7]helicene *rac*-**1** (11.8 mg, 0.0123 mmol, 1.0 equiv) in ether (∼0.3 mL, vacuum transferred) at 0 °C. After 1 h at 0 °C, the reaction vessel was placed in a −30 °C bath, and then the resolving agent (−)-MenthSiCl (0.2 M in ether, 0.037 mmol, 0.18 mL, 3.0 equiv) was added slowly into the reaction mixture at −30 °C. After the addition, the transparent reaction mixture turned turbid. After about 5 min at −30 °C, the reaction vessel was placed in an ice bath for 30 min, and then the reaction mixture was allowed to warm to room temperature overnight. Aqueous workup with ether and chloroform gave the crude product (26.9 mg). A repeat reaction starting from 40.2 mg of [7]helicene *rac*-**1** provided 93.5 mg of crude product. Purification of combined crude product by column chromatography (silica, pentane/benzene, 15:1) gave two fractions F1 and F2.

F1, (−)-7. Yield, 22.6 mg (26%). R_f = 0.40 (pentane/benzene, 15:1). $[\alpha]^{rt}_D$ = −658 (*c* 1.38 × 10^{-3} M, 2.26 mg/mL, cyclohexane). ^{1}H NMR (500 MHz, chloroform-*d*): δ 7.60−7.57 (m, 4H), 7.44−7.36 (m, 10H, overlapped with residual benzene at 7.368 ppm), 7.27−7.13 (m, 6H, overlapped with residual $CHCl_3$), 3.58−3.53 (m, 2H), 3.03−2.82 (m, 8H), 2.48−2.39 (m, 2H), 1.80−1.25 (m, ∼48H, overlapped with residual H_2O), 1.13−1.01 (m, 4H), 0.96−0.71 (m, ∼22H), 0.665 (d, *J* ≈ 8, 6H), 0.317 (d, *J* ≈ 8, 6H). $^{13}C\{^1H\}$ NMR (125 MHz, chloroform-*d*): aromatic region, expected 18 resonances for C_2 point group with diastereotopic phenyl groups; found 18 resonances at δ 143.7, 140.9, 136.4, 136.1, 135.60, 135.56, 134.9, 134.0, 132.9, 130.6, 130.36, 130.32, 129.8, 129.5, 128.5, 128.3 (residual benzene), 128.0, 127.3, 115.8; aliphatic region, expected 24 resonances; found 22 resonances at δ 74.2, 50.2, 45.0, 34.4, 31.95 (overlapped), 31.79, 31.5, 31.1, 30.12, 30.08, 29.92, 29.85, 29.1, 25.1, 22.75, 22.66, 22.51, 22.1, 21.4, 15.3, 14.18, 14.11. IR (ZnSe, cm^{-1}): 3070, 3048, 2954, 2923, 2854 (C−H), 1456, 1429, 1117, 1109, 1066, 1051, 739, 713, 698. UV−vis (cyclohexane): λ_{max}/nm (ε/dm^3 mol^{-1} cm^{-1}) = 194 (8.85 × 10^4), 248 (2.33 × 10^4), 318 (1.10 × 10^4), 339 (1.56 × 10^4), 370 (1.06 × 10^4). CD (cyclohexane): λ_{max}/nm ($\Delta\varepsilon$/dm^3 mol^{-1} cm^{-1}) = 370.2 (−49), 344.6 (−89), 330.8 (−67), 292 (−83), 256 (+55), 234.6 (+70), 205 (+138). HR FABMS (ONPOE matrix): *m*/*z* (ion type, %RA, deviation for the formula): 1631.5658 ([M + 2 + H]$^+$, 100%, 2.5 ppm for $^{12}C_{92}{}^1H_{119}{}^{16}O_2{}^{28}Si_2{}^{32}S_5{}^{79}Br_1{}^{81}Br_1$), 1630.5647 ([M + 2]$^+$, 98%, −1.6 ppm for $^{12}C_{92}{}^1H_{118}{}^{16}O_2{}^{28}Si_2{}^{32}S_5{}^{79}Br_1{}^{81}Br_1$).

F2, (+)-7. Yield, 27.5 mg (31%). R_f = 0.30 (pentane/benzene, 15:1). $[\alpha]^{rt}_D$ = +601 (*c* 2.04 × 10^{-3} M, 2.78 mg/mL, cyclohexane). ^{1}H NMR (500 MHz, chloroform-*d*): δ 7.62−7.60 (m,

4H), 7.46−7.32 (m, 12H), 7.30−7.19 (m, 4H, overlapped with residual $CHCl_3$), 3.45−3.39 (m, 2H), 3.03−2.82 (m, 8H), 2.49−2.41 (m, 2H), 1.81−1.25 (m, ∼48H, overlapped with residual H_2O), 1.13−1.01 (m, 4H), 0.96−0.71 (m, ∼22H), 0.61 (d, J = 6.0, 6H), 0.206 (d, J = 6.8, 6H). $^{13}C\{^1H\}$ NMR (125 MHz, chloroform-*d*): aromatic region, expected 18 resonances for C_2 point group with diastereotopic phenyl groups; found 18 resonances at δ 143.7, 141.0, 136.5, 136.2, 135.7, 135.3, 134.8, 133.65, 133.60, 130.69, 130.64, 130.2 (impurity), 129.96, 129.82, 129.5, 128.4, 127.9, 127.5 115.7; aliphatic region, expected 24 resonances; found 23 resonances at δ 74.1, 50.3, 45.1, 34.4, 31.94, 31.86, 31.79, 31.5, 31.2, 30.23, 30.09, 29.91, 29.83, 29.1, 25.2, 22.74, 22.65, 22.5, 22.1, 21.4, 15.3, 14.18, 14.11. IR (ZnSe, cm^{-1}): 3069, 3048, 2954, 2925, 2856 (C−H), 1456, 1429, 1116, 1082, 1066, 1052, 739, 713, 698. UV−vis (cyclohexane): λ_{max}/nm (ε/dm^3 mol^{-1} cm^{-1}) = 194 (8.66×10^4), 248 (2.19×10^4), 318 (1.03×10^4), 340 (1.47×10^4), 370 (0.97×10^4). CD (cyclohexane): λ_{max}/nm ($\Delta\varepsilon$/dm^3 mol^{-1} cm^{-1}) = 372.2 (+45), 344.8 (+91), 331.2 (+72), 290.8 (+87), 256 (−60), 235.4 (−78), 206 (−146). HR FABMS (ONPOE matrix): m/z (ion type, %RA for m/z = 1628−1636, deviation for the formula): 1630.5629 ($[M + 2]^+$, 100%, −0.5 ppm for $^{12}C_{92}{}^1H_{118}{}^{16}O_2{}^{28}Si_2{}^{32}S_5{}^{79}Br_1{}^{81}Br_1$).

Acknowledgment. This research was supported by the National Science Foundation (CHE-0718117). ChemMatCARS Sector 15 is principally supported by the National Science Foundation/Department of Energy under Grant No. CHE-0087817. The Advanced Photon Source is supported by the U.S. Department of Energy, Basic Energy Sciences, Office of Science, under Contract No. W-31-109-Eng-38.

Supporting Information Available: Complete ref 56, description of experimental detail, and product characterization, including X-ray crystallographic files in CIF format. This material is available free of charge via the Internet at http://pubs.acs.org.